NUCLEAR THEORY, Vol. 29 (2010)
eds. A. Georgieva, N. Minkov, Heron Press, Sofia

Study of ^{6}He+^{12}C Elastic Scattering Using a Microscopic Optical Potential

V. K. Lukyanov[1], **D. N. Kadrev**[2], **E. V. Zemlyanaya**[1], **A. N. Antonov**[2], **K. V. Lukyanov**[1], **M. K. Gaidarov**[2]

[1]Joint Institute for Nuclear Research, Dubna 141980, Russia
[2]Institute for Nuclear Research and Nuclear Energy, Bulgarian Academy of Sciences, Sofia 1784, Bulgaria

Abstract. The ^{6}He+^{12}C elastic scattering data at beam energies of 3, 38.3 and 41.6 MeV/nucleon are studied utilizing the microscopic optical potentials obtained by a double-folding procedure and also by using those inherent in the high-energy approximation. The calculated optical potentials are based on the neutron and proton density distributions of colliding nuclei established in an appropriate model for ^{6}He and obtained from the electron scattering form factors for ^{12}C. The depths of the real and imaginary parts of the microscopic optical potentials are considered as fitting parameters. At low energy the volume optical potentials reproduce sufficiently well the experimental data. At higher energies, generally, additional surface terms having form of a derivative of the imaginary part of the microscopic optical potential are needed. The problem of ambiguity of adjusted optical potentials is resolved requiring the respective volume integrals to obey the determined dependence on the collision energy.

1 Introduction

The availability of radioactive ion beams facilities made it possible in the past decades to carry out many experiments and to get information concerning the structure of exotic light nuclei with a localized nuclear core and a dilute few-neutron halo or skin as well as on the respective reaction mechanisms (for more information see, e.g., the recent review of the problem in Ref. [1]). In this sense, ^{6}He is a typical nucleus having the weak binding energy and extended neutron halo in its periphery. The latter is the reason why in collisions with the proton and nuclear targets the projectile nucleus ^{6}He is breaking up with a comparably large probability that causes the flux loss in the elastic channel. Therefore, the study of elastic scattering of ^{6}He on protons or light targets is a powerful tool to get information on peculiarities of the mechanism of such processes.

The data on cross sections of processes with light exotic nuclei have been analyzed using various phenomenological and microscopic methods. Among the latter we should mention the microscopic analysis using the coordinate-space g-matrix folding method (e.g., Ref. [2] and references therein), as well as works where the real part of the optical potential (ReOP) is microscopically calculated

(e.g., Ref. [3]) using the folding approach (e.g., Refs. [4–7]). Usually the imaginary part of the OP's (ImOP) and the spin-orbit terms have been determined phenomenologically that has led to the usage of a number of fitting parameters. In our previous works [8, 9] instead of using a phenomenological imaginary part of OP we have performed calculations of ^{6}He$+p$ [8] and ^{8}He$+p$ [9] elastic differential cross sections by means of the microscopic OP with the imaginary part taken from the OP derived in [10, 11] in the frameworks of the high-energy approximation (HEA) [12–14] that is known as the Glauber theory. The present work as well as that from Ref. [15] on ^{6}He+^{12}C scattering could give a novel information on mechanism of the process due to the more complicated dependence of the microscopic OP not only on the density of the projectile ^{6}He but also on the density of the target nucleus.

In the last years a number of works has been devoted also to the elastic scattering of ^{6}He on ^{12}C nucleus and, particularly, to the study of the mechanism of this process including the role of breakup channels. In the present paper we perform an analysis of the ^{6}He+^{12}C elastic scattering data at three beam energies $E = 3$ [16], 38.3 [17] and 41.6 MeV/nucleon [18] using the microscopically calculated OP. The data have been already considered individually in the frameworks of other theoretical models. In Ref. [17] the elastic scattering data at $E = 38.3$ MeV/nucleon were analyzed using the semi-microscopic OP. Its real part was defined in a double-folding model including the direct and exchange convolution integrals, while the imaginary part was taken phenomenologically in the WS form. To get a better agreement at larger angles, the dynamic polarization potential (DPP) in the form of a derivative of a WS function was added to the volume OP.

Calculations by coupled reaction channel models [18, 19] with accounting for the cluster and continuum states are encouraged to study their sensitivity to the input information on the reaction mechanism. On the other hand, the breakup reactions reveal themselves through the dynamic polarization terms in the full OP for elastic scattering. The explicit information on these channels can be obtained from the unambiguous OP obtained from the respective analysis of the elastic scattering experimental data. In the present study (see also [15]) we start analyzing the elastic scattering data by the microscopic optical potential obtained in Ref. [10]. Its real part includes the direct and exchange terms that are the same used in Ref. [17]. The imaginary part of OP is based on the Glauber theory of high-energy scattering of complex systems and is an integral which folds the nucleon-nucleon scattering amplitude f_{NN} with the density distribution functions of the bare nucleons of colliding nuclei. Then, we assume that additional terms to our basic OP may be considered as a consequence of the presence of more complicated channels. In the case of the loosely bound ^{6}He projectile these terms are thought to arise due to the breakup channels.

2 The Microscopic Optical Potential

Here we give the main expressions for the real and imaginary parts of the nucleus-nucleus OP

$$U(r) = V^{DF}(r) + iW(r). \tag{1}$$

The real part V^{DF} consists of the direct and exchange double-folding (DF) integrals that include an effective NN potential and density distribution functions of the colliding nuclei:

$$V^{DF}(r) = V^{D}(r) + V^{EX}(r). \tag{2}$$

The formalism of the DF potentials is described in details, e.g., in Refs. [4, 6]. In general, in Eq. (2) V^D and V^{EX} are composed from the isoscalar (IS) and isovector (IV) contributions, but in the considered case the isovector part is omitted because $Z = N$ in the target nucleus ^{12}C and, thus, one can write:

$$V^{D}(r) = \int d^3r_p d^3r_t \rho_p(\mathbf{r}_p)\rho_t(\mathbf{r}_t) v^{D}_{NN}(s), \tag{3}$$

$$V^{EX}(r) = \int d^3r_p d^3r_t \rho_p(\mathbf{r}_p, \mathbf{r}_p + \mathbf{s})\rho_t(\mathbf{r}_t, \mathbf{r}_t - \mathbf{s}) \times v^{EX}_{NN}(s) \exp\left[\frac{i\mathbf{K}(r)\cdot s}{M}\right], \tag{4}$$

where $\mathbf{s} = \mathbf{r} + \mathbf{r}_t - \mathbf{r}_p$ is the vector between two nucleons, one of which belongs to the projectile and another one to the target nucleus. In Eq. (3) $\rho_p(\mathbf{r}_p)$ and $\rho_t(\mathbf{r}_t)$ are the densities of the projectile and the target, respectively. In Eq. (4) $\rho_p(\mathbf{r}_p, \mathbf{r}_p + \mathbf{s})$ and $\rho_t(\mathbf{r}_t, \mathbf{r}_t - \mathbf{s})$ are the density matrices for the projectile and the target that are usually taken in an approximate form [20]. In the modern calculations of the DF potentials the effective interaction v^D_{NN} (of CDM3Y6-type) based on the Paris NN forces and having the form

$$v^{D}_{NN}(E, \rho, s) = g(E)F(\rho)v(s) \tag{5}$$

is usually applied with the distance dependence given by

$$v(s) = \sum_{i=1}^{3} N_i \frac{\exp(-\mu_i s)}{\mu_i s}, \tag{6}$$

and with terms of the energy and density dependencies:

$$g(E) = 1 - 0.003E, \quad F(\rho) = C\Big[1 + \alpha e^{-\beta\rho} - \gamma\rho\Big]. \tag{7}$$

The energy dependent factor in Eq. (7) is taken to be a linear function of the bombarding energy per nucleon, while ρ in $F(\rho)$ is the sum of the projectile and target densities, $\rho = \rho_p + \rho_t$. The parameters N_i, μ_i [Eq. (6)], C, α, β, γ

[Eq. (7)], and all details of the mathematical treatments and calculations are given in Refs. [6, 21].

In Eq. (4) v_{NN}^{EX} is the exchange part of the effective NN interaction. It is important to note that the energy dependence of V^{EX} arises primarily from the contribution of the exponent in the integrand of Eq. (4). Indeed, there the local nucleus-nucleus momentum

$$K(r) = \left\{ \frac{2Mm}{\hbar^2} \left[E - V^{DF}(r) - V_c(r) \right] \right\}^{1/2} \tag{8}$$

with A_p, A_t, m being the projectile and target atomic numbers and the nucleon mass, and $M = A_p A_t/(A_p + A_t)$. As can be seen, $K(r)$ depends on the folding potential $V^{DF}(r)$ that has to be calculated itself and, therefore, we have to deal with a typical non-linear problem. Usually, two different kinds of effective NN potentials are employed in calculations, namely the Paris CDM3Y6 and the Reid DDM3Y1 NN interactions, which are defined by two different sets of the aforementioned parameters. The direct parts of these potentials have different signs and, for example, in the case of CDM3Y6 forces the V^{EX} is negative while V^D is positive. So, if in the calculations one takes only the direct part of V^{DF} with the Paris M3Y NN forces, then the corresponding real part of such OP is positive one. Therefore, one should proceed carefully when neglecting the exchange part of OP.

Concerning the imaginary part of our OP, we take it in two forms. In the first case the imaginary part has the same form as the real one but with different strength. At the same time we test another shape of the imaginary part that corresponds to the full microscopic OP derived in Refs. [10, 11] within the HEA [12, 13]. In the momentum representation this OP has the form

$$U^H(r) = -\frac{E}{k} \bar{\sigma}_N (i + \bar{\alpha}_N) \frac{1}{(2\pi)^3} \int e^{-i\mathbf{qr}} \rho_p(q) \rho_t(q) f_N(q) d^3q. \tag{9}$$

Here $\bar{\sigma}_N$ and $\bar{\alpha}_N$ are the averaged over isospins of nuclei the NN total scattering cross section and the ratio of real to imaginary parts of the forward NN amplitude, both being parameterized, e.g., in Refs. [22, 23]. The NN form factor is taken as $f_N(q) = \exp(-q^2\beta/2)$ with the slope parameter $\beta = 0.219$ fm^2 [24].

Hereafter we shall use only the imaginary part of the full OP (9) transformed (by using the equality $\int d\Omega_q \exp(-i\mathbf{qr}) = 4\pi j_0(qr)$) to the form

$$W^H(r) = -\frac{1}{2\pi^2} \frac{E}{k} \bar{\sigma}_N \int_0^\infty j_0(qr) \rho_p(q) \rho_t(q) f_N(q) q^2 dq. \tag{10}$$

In the further calculations the microscopic volume optical potential has the following form:

$$U(r) = N_R V^{DF}(r) + i N_I W(r), \tag{11}$$

where $W(r)$ is taken to be equal either to $V^{DF}(r)$ or to $W^H(r)$. The parameters N_R and N_I entering Eq. (11) renormalize the strength of OP and are fitted by

comparison with the experimental cross sections. In the present work, attempting to simulate the surface effects caused by the polarization potential [25–27], we add to the volume potential [Eq. (11)] the respective surface terms. Usually, they are taken as a derivative of the imaginary part of OP, as follows:

$$W^{sf}(r) = -iN_I^{sf}\frac{dW(r)}{dr}, \tag{12}$$

$$= -iN_I^{sf} r\frac{dW(r)}{dr}, \tag{13}$$

$$= -iN_I^{sf} r^2\frac{dW(r)}{dr}, \tag{14}$$

$$= -iN_I^{sf}\frac{dW(r-\delta)}{dr}, \tag{15}$$

where N_I^{sf} is also a fitting parameter, δ gives the shift of the potential (15) and in our case is fixed to be $\delta = 1$ fm.

3 Results and Discussion

The results of our work [8] on the ^{6}He+p elastic scattering showed that the large-scale shell model (LSSM) density of ^{6}He microscopically calculated in Ref. [7] using a complete $4\hbar\omega$ shell-model space and the Woods-Saxon single-particle wave function basis with realistic exponential asymptotic behavior is the most preferable one and it is used also in the present work. For ^{12}C we use the symmetrized Fermi-type density with the radius and diffuseness parameters $c = 2.275$ fm and $a = 0.393$ fm from Ref. [28]. They were obtained by defolding the ^{12}C charge density distribution deduced in Ref. [29] from analysis of the corresponding electron scattering form factors.

In Figure 1 are shown the densities of ^{6}He and ^{12}C, as well as the OP's V^{DF} calculated using Eqs. (1)-(7) and W^H obtained within the HEA [Eq. (10)] for the three cases of the incident energy that are considered ($E = 3$, 38.3 and 41.6 MeV/nucleon). It can be seen that the increase of the energy leads to reduced depths and slopes of ReOP and ImOP.

We calculated the ^{6}He+^{12}C elastic scattering differential cross sections using the program DWUCK4 [30] and the microscopically calculated OP's. In the calculations first we use only volume OP (11) for the two types of ImOP (V^{DF} and W^H) and then we add different forms of the surface contributions to the ImOP [Eqs. (12)-(15)]. The latter is done having in mind that due to the breakup channel effects there is a "loss of the flux" from the elastic channel.

We consider the set of the N_i coefficients (N_R, N_I and N_I^{sf}) as parameters to be found out from the comparison with the empirical data. We should mention (as it had been emphasized in our previous works [8, 9] for ^{6,8}He+p scattering) that we do not aim to find a complete agreement with the data. The introduction of the N's related to the depths of the different components of the OP's can be considered as a way to introduce a quantitative measure of the deviations of

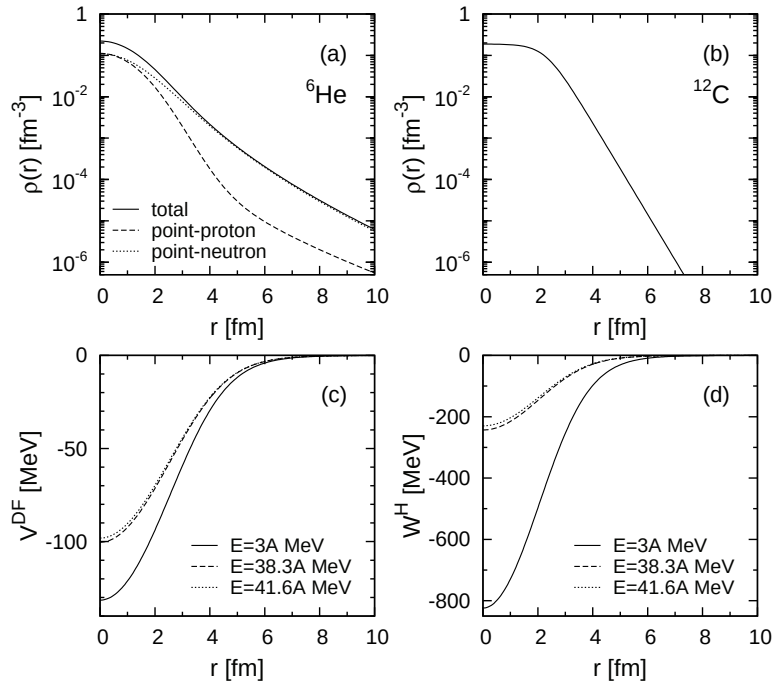

Figure 1. Upper part: total, point-proton and point-neutron microscopic LSSM densities of ^{6}He (from Ref. [7]) (a) and the density of ^{12}C [28, 29] (b). Lower part: microscopic OP's V^{DF} (c) and W^H (d) for the ^{6}He+^{12}C elastic scattering at $E = 3$, 38.3 and 41.6 MeV/nucleon ($N_R = N_I = 1$ and $N_I^{sf} = 0$).

the predictions of our method from the reality (e.g., the differences of N's from unity for given energies).

The results for the energies $E = 38.3$ and 41.6 MeV/nucleon show that the inclusion of different forms of the surface potential leads to almost similar results for the cross section. This was also the case of ^{8}He+p processes studied in our previous work [9]. As is known, the problem of the ambiguity of the values of N's arises when the fitting procedure concerns a limited number of experimental data.

The case of $E = 3$ MeV/nucleon is a particular one because of this rather low energy. Nevertheless, we made an attempt to consider it using OP obtained in our method. The calculations showed that for this energy the fitting procedure led to $N_I^{sf} = 0$ for the case of the surface term given by Eq. (13). We note that in the case of $E = 3$ MeV/nucleon the ambiguity in the explanation of the data [16] still remains.

In what follows, we tried to choose the most physical values of N's for the energies considered. As is known, the fitting procedure belongs to the class of

the ill-posed problems (e.g., Ref. [31]). To resolve this problem it is necessary to impose some physical constraints when fitting the parameters of a model. In our case it might be the data on the total cross sections but often the corresponding values are missing. Another physical criterion that has to be imposed is the obtained potentials to obey a determined behavior of the volume integrals [4]

$$J_V = -\frac{4\pi}{A_p A_t}\int N_R V^{DF}(r) r^2 dr, \quad (16)$$

$$J_W = -\frac{4\pi}{A_p A_t}\int N_I W(r) r^2 dr, \quad (17)$$

as functions of the energy. Indeed, it was shown for nucleon and light-ions scattering on nuclei (see, e.g., Refs. [32–34]) that the values of the volume integrals J_V decrease with the energy increase at $E < 100$ MeV/nucleon, while J_W increases at low energies up to 10-20 MeV/nucleon and then saturates. We would like to note that such conditions were also imposed in Ref. [9] when the microscopic OP's were introduced to study the ^{8}He+p scattering and their depth parameters N_R and N_I were fitted. The values of J_V and J_W for the ^{6}He+^{12}C scattering that fulfil the condition for their energy dependence are presented in Tables 1, 2 and 3. In the cases when we include surface terms to the ImOP we modify J_W accounting for them.

Table 1. The optimal values of the parameters N_R, N_I for the volume OP [Eq. (11)] for the elastic ^{6}He+^{12}C cross sections at energies $E = 3$, 38.3 and 41.6 MeV/nucleon when the imaginary potential W was selected in the forms W^H or V^{DF}. The values of the volume integrals J_V and J_W, χ^2 and total reaction cross sections σ_R (in mb) are also given.

E	W	N_R	N_I	J_V	J_W	χ^2	σ_R
3	W^H	0.826	0.154	297.109	212.952	9.121	1427.33
3	V^{DF}	0.793	0.345	285.239	124.095	9.890	1428.52
38.3	W^H	1.268	0.511	353.442	208.567	80.808	1028.77
38.3	V^{DF}	1.123	0.472	313.025	131.565	50.847	1033.79
41.6	W^H	0.897	0.689	244.933	265.680	3.737	1067.32
41.6	V^{DF}	0.814	0.584	222.269	159.466	3.774	1067.55

Table 2. The same as Table 1 but for the parameters N_R, N_I, and N_I^{sf} of the total OP with the surface term from Eq. (13).

E	W	N_R	N_I	N_I^{sf}	J_V	J_W	χ^2	σ_R
38.3	W^H	1.000	0.023	0.082	278.740	109.172	17.399	1055.67
38.3	V^{DF}	0.924	0.082	0.101	257.556	106.420	5.006	1174.66
41.6	W^H	0.852	0.337	0.051	232.645	188.590	3.734	1070.77
41.6	V^{DF}	0.800	0.500	0.014	218.446	147.876	3.781	1072.40

Table 3. The same as Table 1 but for the parameters N_R, N_I, and N_I^{sf} of the total OP with the surface term from Eq. (14). The values of N_I^{sf} are in fm^{-1}.

E	W	N_R	N_I	N_I^{sf}	J_V	J_W	χ^2	σ_R
3	W^H	0.790	0.074	0.002	284.160	137.506	8.912	1449.98
3	V^{DF}	0.725	0.040	0.008	260.779	55.924	9.418	1533.22
38.3	W^H	0.932	0.028	0.019	259.786	110.017	5.059	1185.22
38.3	V^{DF}	0.932	0.204	0.012	259.786	105.469	8.425	1161.91
41.6	W^H	0.797	0.255	0.011	217.627	152.281	3.711	1091.46
41.6	V^{DF}	0.578	0.041	0.022	157.827	98.546	2.398	1224.91

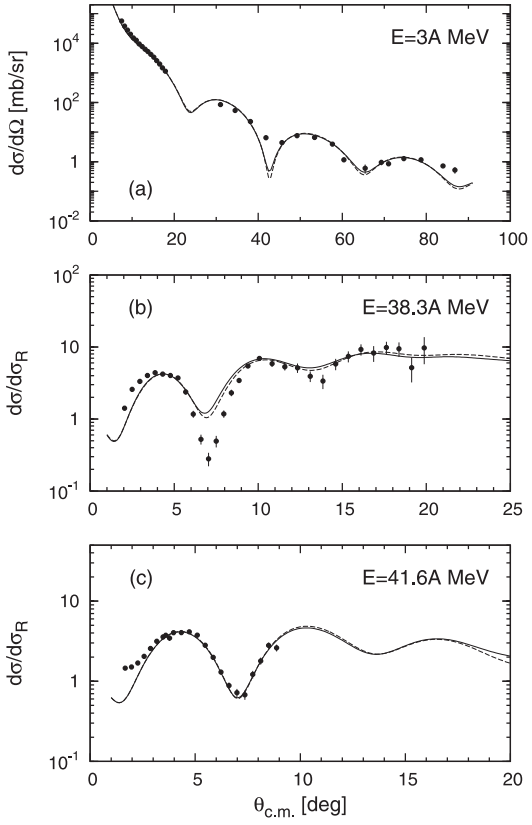

Figure 2. Differential cross section of elastic ^{6}He+^{12}C scattering at $E = 3$ (a), 38.3 (b) and 41.6 MeV/nucleon (c) calculated using only volume OP [Eq. (11)]. Solid line: $W = W^H$, dashed line: $W = V^{DF}$. The values of the fitted parameters N_R and N_I corresponding to the curves in the upper, middle and lower part are given in Table 1. The experimental data are taken from Refs. [16–18].

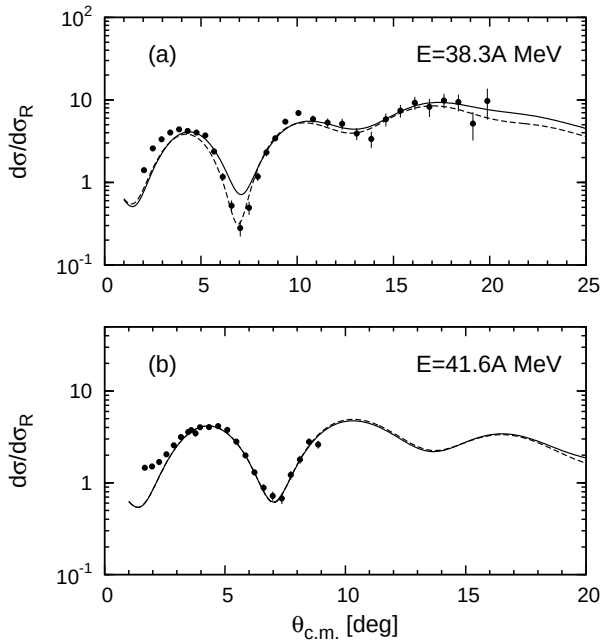

Figure 3. The same as in Figure 2 (without the case for $E = 3$ MeV/nucleon) at $E = 38.3$ (a) and $E = 41.6$ MeV/nucleon (b) calculated using volume OP and surface contribution to the ImOP [Eq. (13)]. The values of the parameters N's are given in Table 2. The experimental data are taken from Refs. [17, 18].

In the next part of the work we select those sets of the parameters N's that lead to the already mentioned behavior of J_V and J_W as functions of the energy for three cases: 1) only the volume terms; 2) the volume terms plus the surface term given by Eq. (13); 3) the volume terms plus the surface term from Eq. (14).

Using the same values of the parameters N's already selected, we present in Figures 2, 3 and 4 the cross sections for the three energies and for the three cases mentioned above. One can see that the best agreement with the data for all the three energies can be obtained by the OP with the volume and surface term [Eq. (14)] whose volume integrals follow (though approximately) the already mentioned energy dependence.

In Figures 5(b) and 5(c) the real and imaginary parts of the OP for $E = 3$ MeV/nucleon obtained in the present work are compared with the phenomenological OP's from Ref. [16] (where WS forms have been used for ReOP and ImOP) and from Ref. [35] (with OP having a squared WS real part and a standard WS shape for the ImOP). The results for the cross sections are shown in Figure 5(a). One can see much better agreement for our cross sections obtained using microscopic OP's than those obtained in a phenomenological way in Refs. [16, 35].

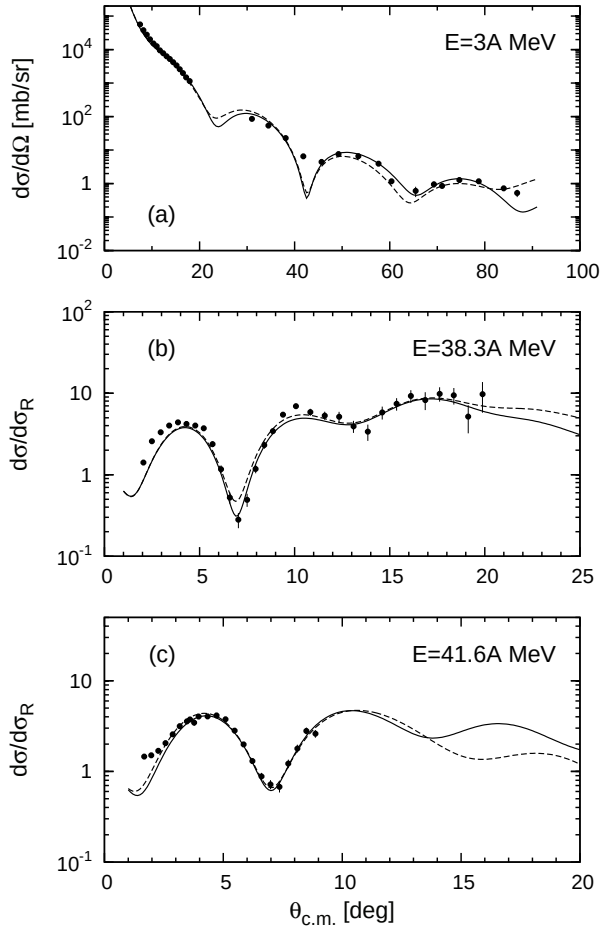

Figure 4. The same as in Figure 2 but for the volume OP and surface contribution to the ImOP [Eq. (14)]. The corresponding N's are given in Table 3. The experimental data are taken from Refs. [16–18].

We should note also that in Ref. [35] the ReOP (V_0) increases and the ImOP (W_0) decreases with the energy increase which is in contradiction with the generally accepted results and with the behavior of the volume integrals as functions of the energy [32–34].

4 Summary and Conclusions

The results of the present work can be summarized as follows:

(i) The microscopic optical potential and cross sections of ^{6}He+^{12}C elastic scattering were calculated at the energies of $E = 3$, 38.3 and 41.6 MeV/nucleon.

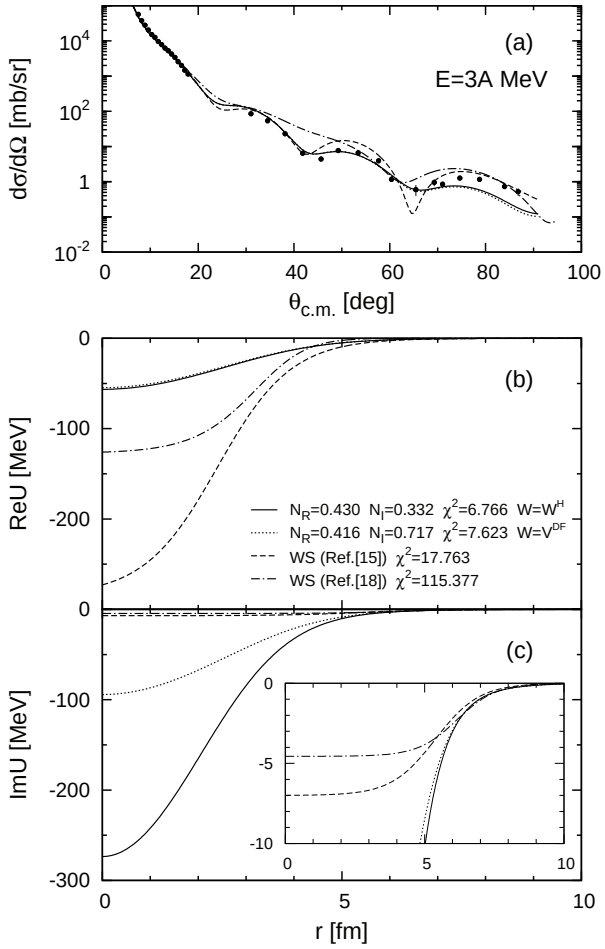

Figure 5. (a) Differential cross section of elastic ^{6}He+^{12} C scattering at $E = 3$ MeV/nucleon. Solid and dotted lines show the results with microscopic ImOP W^H and V^{DF}, respectively. The results with the phenomenological OP's from Refs. [16] and [35] are given by dashed and dash-dotted lines, correspondingly. The experimental data are taken from Ref. [16]; The ReOP and ImOP for $E = 3$ MeV/ nucleon microscopically obtained in the present work (as well as in [15]) and those from Refs. [16] and [35] are given in panels (b) and (c), respectively.

Comparisons with the experimental data and results of other approaches were presented. The direct and exchange parts of the real OP (V^{DF}) were calculated microscopically using the double-folding procedure and density-dependent M3Y (of CDM3Y6-type) effective interaction based on the Paris nucleon-nucleon potential. The imaginary parts of the OP were taken in the forms of V^{DF} or

W^H, the latter being calculated using the high-energy approximation. The microscopic densities of protons and neutrons in ^{6}He calculated within the large-scale shell model were used. The nucleon density distribution functions of ^{12}C were taken as defolded charged densities obtained from the best fit to the experimental form factors from electron elastic scattering on ^{12}C. In this way, in contrast to the phenomenological and semi-microscopic models we deal with fully microscopic approach as a physical ground to account for the single-particle structure of the colliding nuclei. The elastic scattering differential cross sections were calculated using the program DWUCK4.

(ii) While at low energies the volume OP's can reproduce sufficiently well the experimental data, at higher energies additional surface terms in OP having a form of a derivative of the imaginary part of the OP became necessary and were used in the present work.

(iii) The depths of the real and imaginary parts of the microscopic OP's are considered as fitting parameters. As is expected when one utilizes the fitting procedure in the case of a limited number of experimental data, the problem of the ambiguity of these parameters arises. To overcome (at least partly) this ambiguity, additional physical constraints should be imposed. Doing so, we require in our work the values of the depth's parameters N's to lead to volume integrals J_V and J_W with realistic energy dependence for energies $0 < E < 100$ MeV/nucleon. Namely, J_V's must decrease while J_W's increase to some constant values with the increase of the energy.

(iv) The comparison of our results with those of some phenomenological approaches pointed out the advantages of using microscopic real and imaginary parts of the optical potential imposing realistic physical constraints on their depths as that one of the behavior of the volume integrals as functions of the energy.

(v) As in works of other authors (e.g., Ref. [5]) we consider in more details the behavior of the OP in the nuclear periphery. This gives a possibility to make some conclusions about the contributions of the dynamical polarization terms of the OP or, in other words, about the coupled-channel effects.

Acknowledgements

The work is partly supported by the Project from the Agreement for co-operation between the INRNE-BAS (Sofia) and JINR (Dubna). Three of the authors (D.N.K., A.N.A. and M.K.G.) are grateful for the support of the Bulgarian Science Fund under Contract No. 02–285 and one of them (D.N.K.) under Contract No. DID–02/16–17.12.2009. The authors E.V.Z. and K.V.L. thank the Russian Foundation for Basic Research (Grant No. 09-01-00770) for the partial support.

References

[1] N. Keeley, N. Alamanos, K.W. Kemper, and K. Rusek, *Prog. Part. Nucl. Phys*. **63** (2009) 396.

[2] K. Amos, W.A. Richter, S. Karataglidis, and B.A. Brown, *Phys. Rev. Lett*. **96** (2006) 032503; P.K. Deb, B.C. Clark, S. Hama, K. Amos, S. Karataglidis, and E.D. Cooper, *Phys. Rev. C* **72** (2005) 014608.

[3] M. Avrigeanu, G.S. Anagnostatos, A.N. Antonov, and J. Giapitzakis, *Phys. Rev. C* **62** (2000) 017001; M. Avrigeanu, G.S. Anagnostatos, A.N. Antonov, and V. Avrigeanu, *Int. J. Mod. Phys. E* **11** (2002) 249.

[4] G.R. Satchler and W.G. Love, *Phys. Rep*. **55** (1979) 183; G.R. Satchler, *Direct Nuclear Reactions* (Clarendon, Oxford, 1983).

[5] D.T. Khoa and W. von Oertzen, *Phys. Lett. B* **304** (1993) 8; *ibid* **342** (1995) 6; D.T. Khoa, W. von Oertzen, and H.G. Bohlen, *Phys. Rev. C* **49** (1994) 1652; D.T. Khoa, W. von Oertzen and A.A. Ogloblin, *Nucl. Phys*. **A602** (1996) 98; Dao T. Khoa and Hoang Sy Than, *Phys. Rev. C* **71** (2005) 014601; O.M. Knyaz'kov, *Sov. J. Part. Nucl*. **17** (1986) 137.

[6] D.T. Khoa and G.R. Satchler, *Nucl. Phys. A* **668** (2000) 3; D.T. Khoa, G.R. Satchler, and W. von Oertzen, *Phys. Rev. C* **56** (1997) 954.

[7] S. Karataglidis, P.J. Dortmans, K. Amos and C. Bennhold, *Phys. Rev. C* **61** (2000) 024319.

[8] K.V. Lukyanov, V.K. Lukyanov, E.V. Zemlyanaya, A.N. Antonov, and M.K. Gaidarov, *Eur. Phys. J.* **A33** (2007) 389.

[9] V.K. Lukyanov, E.V. Zemlyanaya, K.V. Lukyanov, D.N. Kadrev, A.N. Antonov, M.K. Gaidarov, and S.E. Massen, *Phys. Rev. C* **80** (2009) 024609.

[10] K.V. Lukyanov, E.V. Zemlyanaya, and V.K. Lukyanov, JINR Preprint P4-2004-115, Dubna, 2004; *Phys. At. Nucl*. **69** (2006) 240.

[11] P. Shukla, *Phys. Rev. C* **67** (2003) 054607.

[12] R.J. Glauber, *Lectures in Theoretical Physics* (New York, Interscience, 1959), p.315.

[13] A.G. Sitenko, *Ukr. Fiz. J*. **4** (1959) 152.

[14] W. Czyz and L.C. Maximon, *Ann. Phys*. **52** (1969) 59; J. Formanek, *Nucl. Phys*. **B12** (1969) 441.

[15] V.K. Lukyanov, D.N. Kadrev, E.V. Zemlyanaya, A.N. Antonov, K.V. Lukyanov, and M.K. Gaidarov, *Phys. Rev. C* **82** (2010) 024604.

[16] M. Milin *et al.*, *Nucl. Phys*. **A730** (2004) 285.

[17] V. Lapoux *et al.*, *Phys. Rev. C* **66** (2002) 034608.

[18] J.S. Al-Khalili *et al.*, *Phys. Lett. B* **378** (1996) 45.

[19] T. Matsumoto, T. Egami, K. Ogata, Y. Iseri, M. Kamimura, and M. Yahiro, *Int. J. Mod. Phys. A* **24** (2009) 2191.

[20] J.W. Negele and D. Vautherin, *Phys. Rev. C* **5** (1972) 1472.

[21] K.V. Lukyanov, Comm. JINR, P11-2007-38, Dubna, 2007.

[22] S. Charagi and G. Gupta, *Phys. Rev. C* **41** (1990) 1610; **46** (1992) 1982.

[23] P. Shukla, arXiv:nucl-th/0112039.

[24] G.D. Alkhazov, S.L. Belostotsky, and A.A. Vorobyov, *Phys. Rep*. **42** (1978) 89.

[25] V. Lapoux *et al.*, *Phys. Lett. B* **517** (2001) 18.
[26] D.T. Khoa, G.R. Satchler, and W. von Oertzen, *Phys. Lett. B* **358** (1995) 14.
[27] M. Hussein and G.R. Satchler, *Nucl. Phys*. **A567** (1994) 165.
[28] V.K. Lukyanov, E.V. Zemlyanaya, and B. Słowi'nski, *Phys. At. Nucl.* **67** (2004) 1306.
[29] V.V. Burov and V.K. Lukyanov, P4-11098, JINR, Dubna, (1977); V.V. Burov, D.N. Kadrev, V.K. Lukyanov, and Yu.S. Pol', *Phys. At. Nucl*. **61** (1998) 595.
[30] P.D. Kunz and E. Rost, In: *Computational Nuclear Physics* Vol. 2, edited by K. Langanke *et al.*, Springer-Verlag, New York (1993) p.88.
[31] A.N. Tikhonov and V.Y. Arsenin, *Solutions of Ill-Posed Problems*, V.H. Winston and Sons/Wiley, New York (1977).
[32] E.A. Romanovsky *et al.*, *Bull. Rus. Acad. Sci., Physics*, **62** (1998) 150.
[33] C. Mahaux and H. Ngo, *Nucl. Phys*. **A378** (1982) 205.
[34] M.E. Brandan and G.R. Satchler, *Phys. Rep*. **285** (1997) 143.
[35] Y. Kucuk, I. Boztosun, and T. Topel, *Phys. Rev. C* **80** (2009) 054602.